

CMB Beam Systematics: Impact on Lensing Parameter Estimation

N. J. Miller, M. S. Shimon, B. G. Keating
Center for Astrophysics and Space Sciences, University of California,
San Diego, 9500 Gilman Drive, La Jolla, CA, 92093-0424
(Dated: June 18)

The cosmic microwave background (CMB) is a rich source of cosmological information. Thanks to the simplicity and linearity of the theory of cosmological perturbations, observations of the CMB's polarization and temperature anisotropy can reveal the parameters which describe the contents, structure, and evolution of the cosmos. Temperature anisotropy is necessary but not sufficient to fully mine the CMB of its cosmological information as it is plagued with various parameter degeneracies. Fortunately, CMB polarization breaks many of these degeneracies and adds new information and increased precision. Of particular interest is the CMB's B-mode polarization which provides a handle on several cosmological parameters most notably the tensor-to-scalar ratio, r , and is sensitive to parameters which govern the growth of large scale structure (LSS) and evolution of the gravitational potential. These include CMB temperature anisotropy and C-to-B-mode polarization conversion via gravitational lensing. However, both primary gravitational-wave- and secondary lensing-induced B-mode signals are very weak and therefore prone to various foregrounds and systematics. In this work we use Fisher-matrix-based estimations and apply, for the first time, Monte-Carlo Markov Chain (MCMC) simulations to determine the effect of beam systematics on the inferred cosmological parameters from upcoming experiments: PLANCK, POLARBEAR, SPIDER, QUIET+CLOVER and CMBPOL. We consider beam systematics which couple the beam substructure to the gradient of temperature anisotropy and polarization (differential beam width, pointing and ellipticity) and beam systematics due to differential beam normalization (differential gain) and orientation (beam rotation) of the polarization-sensitive axes (the latter two effects are insensitive to the beam substructure). We determine allowable levels of beam systematics for given tolerances on the induced parameter errors and check for possible biases in the inferred parameters concomitant with potential increases in the statistical uncertainty. All our results are scaled to the 'worst case scenario'. In this case and for our tolerance levels the beam rotation should not exceed the few-degree to sub-degree level, typical ellipticity is required to be 1% level, the differential gain allowed level is a few parts in 10^3 to 10^4 , differential beam width upper limits are of the sub-percent level and differential pointing should not exceed the few- to sub-arcsec level.

PACS numbers: 98.70.Vc

INTRODUCTION

The standard cosmological model accounts for a multitude of phenomena occurring over decades of length and angular scales throughout the entire history of cosmological evolution. Remarkably, doing so only requires about a dozen parameters. Perhaps one of the most useful cosmological probes is cosmic microwave background (CMB) temperature anisotropy whose physics is well understood. Complementary cosmological probes can assist in breaking some of the degeneracies inherent in the CMB and further tighten the constraints on the inferred cosmological parameters. Temperature anisotropy alone cannot capture all the cosmological information in the CMB, and its polarization probes new directions in parameter space. B-mode polarization observations are noise-dominated but the robust secondary signal associated with gravitational lensing, which is known up to an uncertainty factor of two on all relevant scales, is at the threshold of detection by upcoming CMB experiments. The lensing signal may have been detected already through its

signature on the CMB anisotropy as reported recently by ACBAR (Reichardt et al. [1]). Lensing by the large scale structure (LSS) also converts primary E-mode to secondary B-mode. When high fidelity B-mode data are available a wealth of information from the inflationary era (Zaldarriaga & Seljak [2], Kamionkowski, Kosowsky & Stebbins [3]), and cosmological parameters that control the evolution of small scale density perturbations (such as the running of the spectral index of primary density perturbations, neutrino mass and dark energy equation of state), will be extracted from the CMB. At best, B-mode polarization from lensing is a factor of three times smaller than the primary E-mode polarization, so it is prone to contamination by both astrophysical foregrounds and instrumental systematics. It is mandatory to account for, and remove when possible, all sources of spurious B-mode in analyzing upcoming CMB data, especially those generated by temperature leakage due to beam mismatch, since temperature anisotropy is several orders of magnitude larger than the expected B-mode level produced by lensing.

Beam systematics have been discussed extensively (Hu, Hedman & Zaldarriaga [4], Rosset et al. [5], O’Dea, Challinor & Johnson [6], Shim on et al. [7]). All the effects are associated with beam imperfections or beam mismatch in dual beam experiments, i.e. where the polarization is obtained by differencing two signals which are measured simultaneously by two beams with two orthogonal polarization axes. Fortunately, several of these effects (e.g. differential gain, differential beam width and the first order pointing error – ‘dipole’; Hu, Hedman & Zaldarriaga [4], O’Dea, Challinor & Johnson [6], Shim on et al. [7]) are reducible with an ideal scanning strategy and otherwise can be cleaned from the dataset by virtue of their non-quadrupolar nature which distinguishes them from genuine CMB polarization signals. Other spurious polarization signals, such as those due to differential ellipticity of the beam, second order pointing errors and differential rotation, persist even in the case of ideal scanning strategy and perfectly mimetic CMB polarization. These represent the minimal spurious B-mode signal, residuals which will plague every polarization experiment. We refer to them in the following as ‘irreducible beam systematics’.

To calculate the effect of beam systematics we invoke the Fisher information-matrix formalism as well as Monte Carlo simulations of parameter extraction. Our objective is to determine the susceptibility of the above mentioned, and other, cosmological parameters to beam systematics. For the Fisher-matrix-based method and the Monte Carlo simulations we calculate the underlying power spectrum using CAMB (Lewis, Challinor & Lasenby [8]). The Monte-Carlo simulations are carried out with COSMOMC (Lewis & Bridle [9]). We represent the extra noise due to beam systematics by analytic approximations (Shim on et al. [7]) and include lensing extraction in the parameter inference process, following Kaplinghat, Knox & Song [10] and Lesgourgues et al. [11] (see also Perotto et al. [12] for the Monte Carlo simulations) for neutrino mass (and other cosmological parameters) inference from CMB data.

This paper illustrates the effect of beam systematics and its propagation to parameter estimation and error forecasts for upcoming experiments. Our main concern is the effect on the following cosmological parameters: the tensor-to-scalar ratio r , the total neutrino mass M (assuming three degenerate species), tilt of the scalar index n_s , dark energy equation of state w , and the spatial curvature, Ω_k . The lensing-induced B-mode signal is sensitive to all parameters (except the tensor-to-scalar ratio) and peaks at few arcminute scales, while the tensor-to-scalar ratio depends on the energy scale of inflation and the primordial signal peaks at the characteristic horizon size at last scattering, $\sim 2^\circ$. We note that while the LSS-induced and primordial tensor power B-mode spectra are sub- K the shape of the primordial B-mode spectrum is known (only its amplitude is unknown, Keating [13]) and

the secondary LSS-induced B-mode is guaranteed to exist by virtue of the known existence of LSS and E-mode polarization.

The paper is organized as follows. We describe the formalism of beam systematics for general non-gaussian beams and provide a cursory description of a critical tool to mitigate polarization systematics – a half wave plate (HWP), in section 2. The effect of lensing on parameter extraction within the standard quadratic-estimators formalism is discussed in section 3. The essentials of the Fisher matrix formalism are given in section 4 as well as some details on the Monte Carlo simulations invoked here. Our results are described in section 5 and we conclude with a discussion of our main findings in section 6.

BEAM SYSTEMATICS

Beam systematics due to optical imperfections depend on both the underlying sky, the properties of the polarimeter and on the scanning strategy. A constructive example is the effect of differential pointing. This effect depends on the temperature gradient to first order. The rms CMB temperature gradients at the 1° , 30° , 10° , 5° and 1° scales are 1.4 , 1.5 , 3.5 , 2.5 and 0.2 K=arcmin, respectively. Therefore, any temperature difference measured with a dual beam experiment (with typical beam width few arcminutes) with a 1° pointing error will result in a 1 K systematic polarization which has the potential to contaminate the B-mode signal. Similarly, the systematic induced by differential ellipticity results from the variation of the underlying temperature anisotropy along the two polarization-sensitive directions which, in general, differ in scale depending on the mean beam width, degree of ellipticity and the tilt of the polarization-sensitive direction with respect to the ellipse’s principal axes. For example, the temperature difference measured along the major and minor axes of a 1° beam with a 2% ellipticity scales as the second gradient of the underlying temperature which on this scale is 0.2 K=arcmin² and the associated induced polarization is therefore expected to be on the ~ 1 K level. The spurious signals due to pointing error, differential beam width and beam ellipticity all peak at angular scales comparable to the beam size. If the beam size is $\sim 1^\circ$ the beam systematics mainly affect the deduced tensor-to-scalar ratio, r . If the polarimeter’s beam width is a few arcminutes the associated systematics will impact the measured neutrino mass m_ν , spatial curvature Ω_k , running of the scalar spectral index n_s and the dark energy equation of state w (which strongly affects the lensing-induced B-mode signal). It can certainly be the case that other cosmological parameters will be affected as well. Two other spurious polarization signals we explore are due to differential gain and differential rotation; these ef-

fects are associated with different beam normalizations and orientation, respectively, and are independent of the coupling between beam substructure and the underlying temperature perturbations. In particular, they have the same scale dependence as the primordial temperature anisotropy and polarization power spectra, respectively, and their peak impact will be on scales associated with the CMB's temperature anisotropy ($l \sim 1$) and polarization ($l \sim 10^0$).

Mathematical Formalism

We work entirely in Fourier space and in this section we generalize our results (Shimon et al. [7]) to the case of the most general beam shapes. Although the tolerance levels on the beam parameters we derive in sections 4 and 5 are based on the assumption of elliptical beams, they can be easily generalized to arbitrary beam shape, given the beam profile, as we describe below. This can be used to adopt our results to actual measured beam maps incorporating other classes of beam nonideality such as sidelobes.

We expand the temperature anisotropy and Q and U Stokes parameters in 2-D plane waves since for sub-beam scales this is a good approximation. While the (spin-0) temperature anisotropy is expanded in scalar plane waves $e^{i\mathbf{l}\cdot\mathbf{r}}$, the (spin-2) polarization tensor $Q + iU$ is expanded in tensor plane waves $e^{i\mathbf{l}\cdot\mathbf{r}} e^{2i(\phi - \psi)}$. Since in real space the temperature and polarization fields are convolved with the polarimeter's beams, these expressions are simply the product of their Fourier transforms in Fourier space. For a general beam $B(\mathbf{r})$, the measured 2D polarized beam map, may exhibit a pointing error. In this case, the Fourier transform of the beam function acquires a phase

$$\tilde{B}(\mathbf{l}) = \tilde{B}(\mathbf{l}) \exp(i\mathbf{l}\cdot\boldsymbol{\delta}): \quad (1)$$

It is useful to switch to polar coordinates at this point, where we define

$$\begin{aligned} l_x &= l \cos(\phi + \delta) \\ l_y &= l \sin(\phi + \delta) \\ x &= r \cos \psi \\ y &= r \sin \psi \end{aligned} \quad (2)$$

and $\phi + \delta$ is the angle of the polarization axis in a coordinate system fixed to the sky (Fig. 1 of Shimon et al. [7]). The Fourier representation of an arbitrary beam then becomes

$$\begin{aligned} \tilde{B}(\mathbf{l}) &= \int_{\mathcal{D}} B(\mathbf{r}) e^{i\mathbf{l}\cdot\mathbf{r}} d^2r \\ &= \int_{\mathcal{D}} B(\mathbf{r}) e^{i\mathbf{l}r \cos(\phi + \delta - \psi) + i\mathbf{l}r \sin(\phi + \delta - \psi)} d^2r \\ &= \int_{\mathcal{D}} \int_{m,n} B_{m,n}(\mathbf{l}) e^{i(m+n)(\phi + \delta - \psi)} \end{aligned} \quad (3)$$

where

$$B_{m,n}(\mathbf{l}) = \int_{\mathcal{D}} J_m(\mathbf{l}r) J_n(\mathbf{l}r) e^{i(m+n)(\phi + \delta - \psi)} r dr \quad (4)$$

and in the last step we employed the expansion of 2-D plane waves in terms of cylindrical Bessel functions

$$e^{i\mathbf{l}\cdot\cos(\phi + \delta - \psi)} = \sum_{n=-\infty}^{\infty} i^n J_n(\mathbf{l}r) e^{in(\phi + \delta - \psi)}; \quad (5)$$

As in Shimon et al. [7], the optimal map constructed from the CMB data depends on the measurements as

$$\mathbf{m}(\mathbf{p}) = \begin{pmatrix} 0 & \dots & 0 \\ \sum_{t;j \in \mathcal{P}} \mathbf{A}_j^T(\mathbf{p};t) \mathbf{A}_j(\mathbf{p};t) \mathbf{A} \\ 0 & \dots & 0 \\ \sum_{t;j \in \mathcal{P}} \mathbf{A}_j^T(\mathbf{p};t) \mathbf{d}_j(\mathbf{p};t) \mathbf{A} \end{pmatrix} \quad (6)$$

where the sums run over all measurements of the pixel \mathbf{p} . The pointing vector \mathbf{A} is given by

$$\mathbf{A} = \begin{pmatrix} 1 \\ \frac{1}{2} e^{2i(\phi + \delta - \psi)} \\ \frac{1}{2} e^{-2i(\phi + \delta - \psi)} \end{pmatrix}; \quad (7)$$

is a function of both the pixel \mathbf{p} and t , and \mathbf{A}^T is \mathbf{A} transposed. Once the leading beam coefficients $B_{m,n}(\mathbf{l})$ have been calculated, the induced power spectra of the systematics can be calculated according to Eqs. (24), (33), (A.1) and (A.2) of Shimon et al. [7].

Several of the beam systematics can be mitigated by employing a rotating half wave plate (HWP) polarization modulator (e.g. Hanany et al. [14], Johnson et al. [15], MacTavish et al. [16]). These can operate in continuous or stepped rotation. When HWP modulators are included we replace the above scanning angle $(\phi + \delta - \psi)$ with $(\phi + \delta - \psi) + 2't$ where $'$ is the angular velocity of the HWP (O'Dea, Challinor & Johnson [6]). Our deduced tolerance levels given below are presented in a fashion independent of the details of the scanning strategy; all the information about the scanning strategy is encapsulated in the functions f_1 and f_2 :

$$\begin{aligned} f_1 &= \frac{1}{2} \mathfrak{F}_+((1;0))^2 \\ f_2 &= \frac{1}{2} \mathfrak{F}_+((1;-1))^2 + \frac{1}{2} \mathfrak{F}_+((1;1))^2 \end{aligned} \quad (8)$$

where

$$\begin{aligned} \mathfrak{F}(\mathbf{m};n) &= \int_{\mathcal{D}} h e^{i(2m+n)(\phi + \delta - \psi)} d\mathbf{l} \\ \mathfrak{H}(\mathbf{m};n) &= \frac{1}{D} [\mathfrak{F}(\mathbf{m};n) - \mathfrak{F}(\mathbf{m}-2;n) h e^{4i(\phi + \delta - \psi)}] \\ D &= \int_{\mathcal{D}} h e^{i4(\phi + \delta - \psi)} d\mathbf{l} \end{aligned} \quad (9)$$

and the angular brackets in $\langle \dots \rangle_i$ represent average over measurements of a single pixel p , averaged over time. In these averages $\langle \dots \rangle_i \equiv \langle \dots \rangle_{(p;t) \pm 2't}$, and therefore even if the scanning strategy does not uniformly cover all polarization angles of a given spatial pixel, the HWP mitigates the spurious polarization caused by beam systematic effects if integrated over long time intervals.

At this point, it is instructive to show how, in case of ideal scanning strategy, the first order pointing effect vanishes. As can be seen from Table II this effect involves a convolution of the beam function and underlying temperature anisotropy power spectrum with f_2 in multipole space. From the above definitions

$$\begin{aligned} h_+(\ell; 1) &= \int d\Omega \langle h_e^{3i} \rangle_i \langle h_e^i \rangle_i h_e^{4i} \\ h_+(\ell; 1) &= \int d\Omega \langle h_e^i \rangle_i \langle h_e^{3i} \rangle_i h_e^{4i} \end{aligned} \quad (10)$$

and therefore if with each scanning angle there is associated an angle $\pm 180^\circ$ the f_2 (Eqs. 8 and 10) vanishes in real space and so does its Fourier transform. Note that even if the scanning strategy is non-ideal f_2 will vanish provided that for each angle the angle $\pm 180^\circ$ is sampled the same number of times per pixel. This suggests that the dipole systematic can be removed altogether by removing all data points that contribute to $h_+(\ell; 1)$ and $h_+(\ell; 1)$, i.e. those measurements at θ for which $\theta \pm 180^\circ$ is not sampled. Similar considerations apply to f_1 which controls the level of the differential beam width and differential gain-induced systematics (see Table II).

Simplifying Scan Strategy Effects

When the polarization angle at each pixel on the sky is uniformly sampled the average $\langle h_e^{in} \rangle_i$ vanishes for every $n \neq 0$. In this case the scanning strategy is referred to as an ideal scanning strategy. For uniform, but non-ideal, scanning strategies, the scanning functions f_1 and f_2 mentioned above (which are combinations of $\langle h_e^{in} \rangle_i$) are non-vanishing even when $n > 0$ but uniform in real space. As a result their Fourier transforms are unnormalized delta-functions (the actual amplitudes are directly related to the average values $\langle h_e^{in} \rangle_i$), and the convolutions in Fourier space shown in Tables III-IV of Shim on et al. [7] become trivial. To determine the tolerance level for beam parameters we assume such uniform scanning strategies. Even if the scanning strategy is not strictly uniform, as long as it can be reasonably approximated by a sum over a few lowest multipoles such as

$$f_i(\ell) = \sum_{\ell=0}^{\ell_{max}} f_i^0(\ell^0) (\ell - \ell^0) = (\ell - \ell^0) \quad (11)$$

(where ℓ_{max} is sufficiently small, and $i = 1$ or 2 , where f_1 and f_2 are defined in Eq. 8), then the ℓ mode mixing due to the convolution of the underlying power spectra

and the scanning functions as in Table II (\otimes stands for convolution in multipole space)

$$f_i \otimes C_1^T = \frac{f_i}{2} \otimes C_1^T \quad (12)$$

where $f_i = \sum_{\ell=0}^{\ell_{max}} f_i(\ell)$ and we assume here that the nonvanishing multipoles of f_i are concentrated near 0, i.e. that the scanning strategy is non-ideal, yet approximately uniform. We have employed this simplifying assumption throughout.

THE EFFECT OF SYSTEMATICS ON LENSING RECONSTRUCTION

Gravitational lensing of the CMB is both a nuisance and a valuable cosmological tool (e.g. Zaldarriaga & Seljak [17]). It certainly has the potential to complicate CMB data analysis due to the non-gaussianity it induces. However, it is also a unique probe of the growth of structure in the linear, and mildly non-linear, regimes (redshift of a few). Kaplinghat, Knox & Song [10], Lesgourgues et al. [11], as well as others, have shown that with a nearly ideal CMB experiment, neutrino mass limits can be improved by a factor of approximately four by including lensing extraction in the data analysis using CMB data alone. This lensing extraction process is not perfect; a fundamental residual noise will affect any experiment, even ideal ones. This noise will, in principle, propagate to the inferred cosmological parameters if the latter significantly depend on lensing extraction, e.g. neutrino mass, and w . It is important to illustrate first the effect of beam systematics on lensing reconstruction. By optimally filtering the temperature and polarization Hu & Okamoto [18] reconstructed the lensing potential from quadratic estimators. It was shown that for experiments with ten times higher sensitivity than Planck, the EB estimator yields the tightest limits on the lensing potential. This result assumes no beam systematics which might significantly contaminate the observed B-mode.

We illustrate the effect of differential beam rotation, ellipticity and differential pointing (see Shim on et al. [7]) on the noise of lensing reconstruction with POLAR-BEAR (1200 detectors), CMBPOL-A (one of two toy experiments we consider for CMBPOL; 0.22 K sensitivity and 5' beam) and a toy model considered earlier by O'Dea, Challinor & Johnson [6] which we refer to as QUET+CLOVER in Figures 1, 2 and 3, respectively. These are perhaps the most pernicious systematics. Beam rotation induces cross-polarization which leaks the much larger E-mode to B-mode polarization and differential ellipticity leaks T to B. Both leak to B-mode in a way indistinguishable under rotation from a true B-mode signal. The rotation and ellipticity parameters (θ and e , respectively) we considered range from 0.01 to 0.20 (e is dimensionless and θ is given in radians). The

differential pointing ϵ , was set to 1% and 10% of the beam width while the dipole and octupole components of the scanning strategy were set to the 'worst case scenario' $f_2 = 1$, i.e. the unlikely situation where all hits at a given pixel takes place at the same polarization angle (again, for ideal scanning strategy $f_2 = 0$ and the dipole effect due to differential pointing vanishes). Note for POLARBEAR (Figure 1) with $\epsilon = 0.2^\circ$ the lensing potential can be reconstructed up to $l \approx 200$, while with no beam rotation it can be reconstructed up to $l \approx 250$. However, with CM BPOL-A (Figure 2) lensing reconstruction degrades significantly in the presence of beam rotation [from good reconstruction up to $l \approx 600$ in the systematics-free case down to $l \approx 250$ when $\epsilon = 0.2^\circ$ and $\theta = 0.5^\circ$ (in case $f_2 = 1$)]. The reason for the qualitative difference is that for experiments with sensitivities comparable to PLANCK or POLARBEAR, the best estimator of the lensing potential comes from the TT or TE correlations and the cross-correlations involving B-mode are only secondary in probative power (see top left panel of Figure 1). Therefore, lensing reconstruction for these experiments is hardly affected by beam systematics (we ignored the negligible beam systematics' effect on temperature anisotropy and considered only those of E and B). In contrast, as can be seen from Figure 2, CM BPOL-A's lensing reconstruction is significantly degraded since its lensing reconstruction is dominated by the contribution of the EB estimator for all relevant multipoles (see top left panel of Figure 2). The modified noise in reconstructing the lensing potential, N_1^{dd} , is consistently substituted into our Fisher matrix and Monte Carlo simulations (below, we summarize the relevant expressions of the quadratic estimators method).

Following Hu & Okamoto [18] the MV noise on the lensing deflection angle reconstructed power spectrum C_1^{dd} is

$$N_{M_V}^{\text{dd}} = 4 \sum_{\ell} (N^{-1})_{\ell}^2 \quad (13)$$

where

$$N_{\ell}^{-1}(\ell) = L^2 A_{\ell}(\ell) A_{\ell}(\ell) \sum_{\ell_1, \ell_2} \frac{d^2 h_{\ell_1}}{(2\ell_1)^2} F_{\ell_1}(\ell_1; \ell_2) F_{\ell_2}(\ell_1; \ell_2) C_{\ell_1}^{x^0; x^0} C_{\ell_2}^{x^0; x^0} + F_{\ell_2}(\ell_2; \ell_1) C_{\ell_1}^{x^0; x^0} C_{\ell_2}^{x^0; x^0} A_{\ell}(\ell) = L^2 \sum_{\ell_1, \ell_2} \frac{d^2 h_{\ell_1}}{(2\ell_1)^2} h_{\ell_1}(\ell_1; \ell_1) F_{\ell_1}(\ell_1; \ell_1) \quad (14)$$

and ℓ stands for one of the pairings TT, TE, EE, TB and EB (BB does not participate in these combinations). The coupling takes place between different modes ℓ_1 and ℓ_2 . When $\ell = \text{TT or EE}$

$$F_{\ell_1}(\ell_1; \ell_2) = \frac{h_{\ell_1}(\ell_1; \ell_2)}{2C_{\ell_1}^{x^0; x^0} C_{\ell_2}^{x^0; x^0}}; \quad (15)$$

and when $\ell = \text{TB or EB}$

$$F_{\ell_1}(\ell_1; \ell_2) = \frac{h_{\ell_1}(\ell_1; \ell_2)}{C_{\ell_1}^{0; x^0} C_{\ell_2}^{x^0; 0}} \quad (16)$$

where C_{ℓ}^0 are the observed power spectra, i.e. including lensing, main-beam dilution on small scales, and in principle - beam systematics (see Tables I and II). The latter mainly affect the B-mode polarization, and as a result, the EB estimator. A list of $h_{\ell_1}(\ell_1; \ell_2)$ can be found in Hu & Okamoto [18]. We have used the publically available code [19] employed in Lesgourgues et al. [11] and in Perotto et al. [12]. The code is based on the formalism developed in Okamoto & Hu [20], an extension of Hu & Okamoto [18] to the full-sky, to calculate the noise level in lensing reconstruction.

ERROR FORECAST

Accounting for beam systematics in both Stokes parameters and lensing power spectra is straightforward. In addition, the instrumental noise associated with the main beam is accounted for, as is conventional, by adding an exponential noise term. Assuming gaussian white noise

$$N_1 = \frac{1}{a (N_1^{\text{aa}})^{-1}} \quad (17)$$

where a runs over the experiment's frequency bands. The noise in channel a is (assuming a gaussian beam)

$$N_1^{\text{aa}} = (a_{\text{beam}})^2 e^{-1/(1+\theta)^2 a^2} = 8 \ln(2); \quad (18)$$

where a_{beam} is the noise per pixel in K-arcmin, a is the beam width (see Table III), and we assume noise from different channels is uncorrelated. The power spectrum then becomes

$$C_1^X = C_1^X + N_1^X \quad (19)$$

where X is either the auto-correlations TT, EE and BB or the cross-correlations TE, TB and EB (the latter two power spectra vanish in the standard model but not in the presence of beam systematics and exotic parity-violating physics e.g. Carroll [21], Liu, Lee & Ng [22], Xia et al. [23], Komatsu et al. [24] or primordial magnetic fields e.g. Kosowsky & Loeb [25]). For the cross-correlations, the N_1^X vanish as there is no correlation between the instrumental noise of the temperature and polarization (in the absence of beam systematics).

Fisher-Matrix-Based Calculation

The effect of instrumental noise is simply to increase the error bars, which is evident from the Fisher matrix

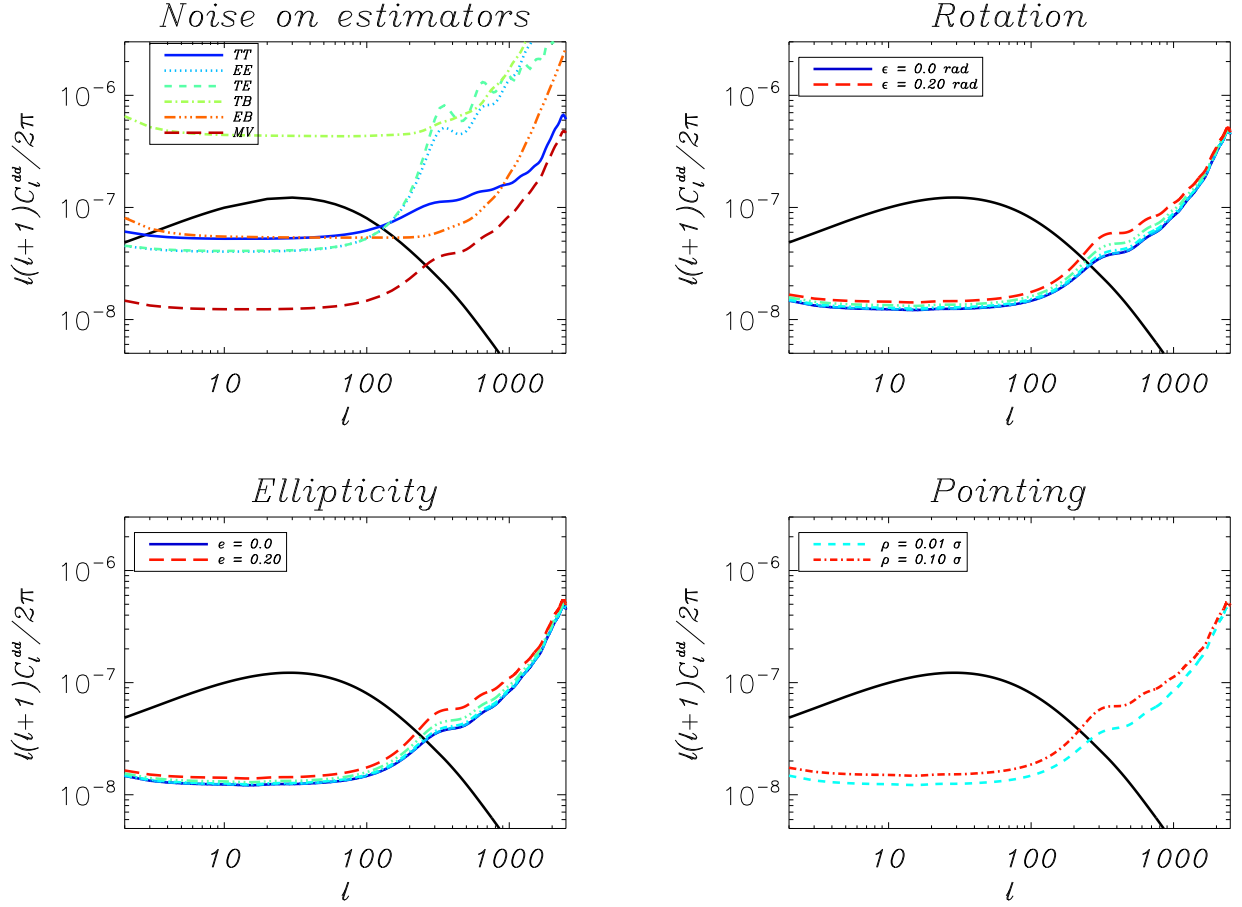


FIG. 1: For all panels the solid black curve is the detection angle power spectrum C_l^{dd} caused by gravitational lensing by the LSS. Top left: The noise (with no systematics) in lensing-reconstruction from the quadratic optimal filters for POLARBEAR TT (solid dark blue), EE (dot light blue), TE (dashed green), TB (dot-dash yellow), EB (double-dot-dash orange) and MV (dashed dark red). Top right: Noise in lensing reconstruction for POLARBEAR with the MV estimator including the effects of the most pernicious irreducible cross-polarization systematic: differential rotation. Differential rotation values are (bottom to top) $\epsilon = 0.01, 0.02, 0.05, 0.10$ and 0.20 radian, respectively. High signal-to-noise detection angle reconstruction can be obtained over nearly a decade of angular scale. For POLARBEAR sensitivity and angular resolution, the lowest-noise estimator comes from correlations of the temperature only. This explains why even an extremely large beam rotation $\epsilon = 0.2$ results in only a small increase in the lensing reconstruction's noise level. Bottom left: Noise in lensing reconstruction for POLARBEAR with the MV estimator including the most pernicious irreducible instrumental polarization systematics: differential ellipticity. Differential ellipticity values are (bottom to top) $e = 0.01, 0.02, 0.05$ and 0.10 , respectively (we assume $e = 45^\circ$). The same explanation for insensitivity to differential rotation applies here for differential ellipticity e ; the best estimator for this experiment is derived from temperature correlations which are hardly affected by beam systematics (and completely ignored in this analysis). Bottom right: Noise in lensing reconstruction for POLARBEAR with the MV estimator for the most pernicious reducible instrumental polarization systematics: differential pointing with 1% and 10% pointing errors (i.e. $\rho = 0.01$ and $\rho = 0.1$, respectively) under the 'worst case' assumption that the scanning-strategy-related function $f_2 = 1$.

formalism below. The 1- σ error (δ_i) on the cosmological parameter θ_i can be read-off from the appropriate diagonal element of the inverse Fisher matrix

$$(\delta_i) = \sqrt{\frac{1}{(F^{-1})_{ii}}} \quad (20)$$

where the Fisher matrix elements are defined as

$$F_{ij} = \frac{D}{\theta_i \theta_j} \frac{\partial^2 \mathcal{L}}{\partial \theta_i \partial \theta_j} \quad (21)$$

\mathcal{L} is the likelihood function, and Eq. (21) is evaluated at the best-fit point in parameter space. Explicitly, the Fisher matrix elements for the CMB read

$$F_{ij} = \frac{1}{2} \sum_{l=1}^X (2l+1) f_{\text{sky}} \text{Trace} \left[C^{-1} \frac{\partial C}{\partial \theta_i} C^{-1} \frac{\partial C}{\partial \theta_j} \right] \quad (22)$$

The pre-factor $\frac{1}{2} (2l+1) f_{\text{sky}}$ comes from the sample-variance of the multipole l with an experiment covering

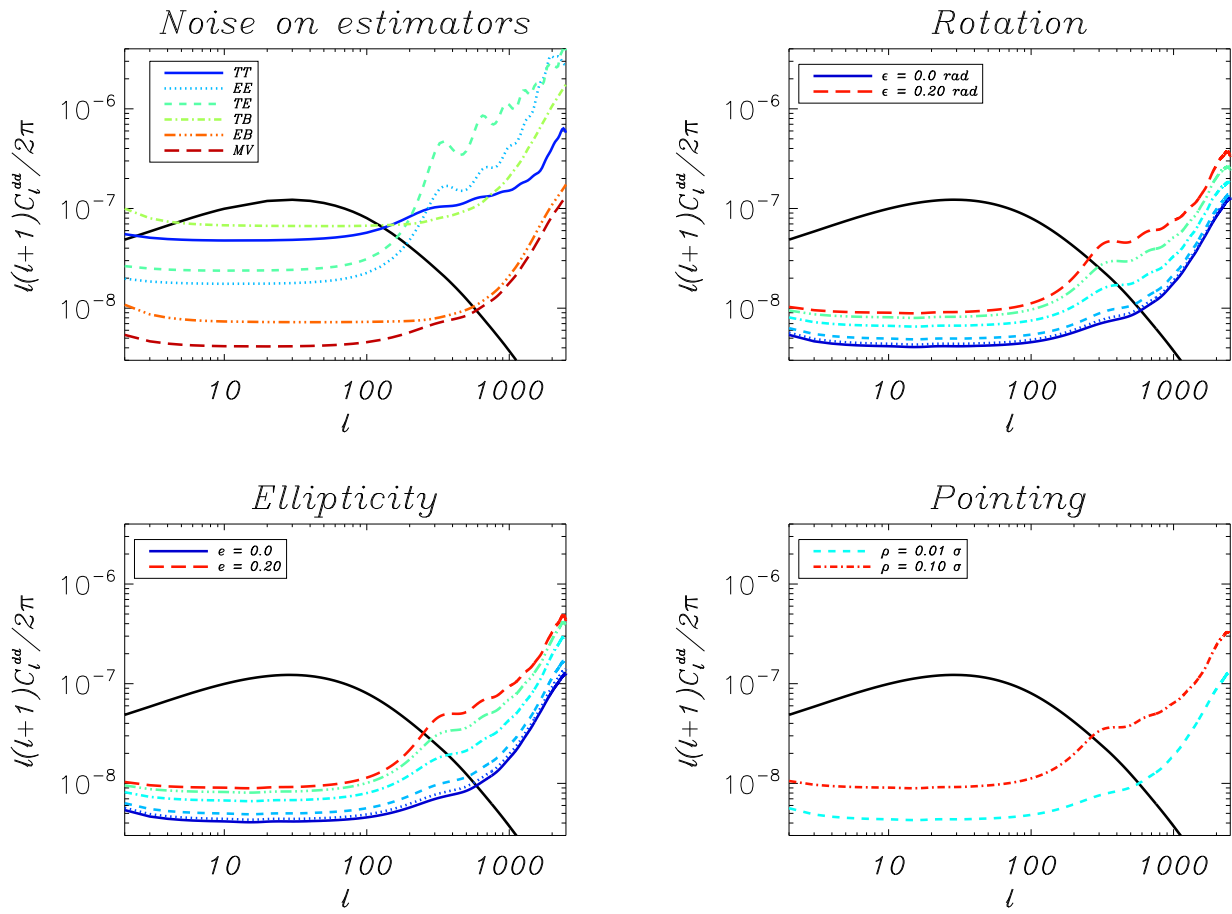


FIG. 2: Lensing reconstruction with CMBPOL-A: As in Figure 1. For CMBPOL-A sensitivity and angular resolution, the lowest-noise estimator comes from correlations of the EB estimator. Therefore, lensing reconstruction is significantly affected by beam systematics.

a fraction f_{sky} of the sky. The matrix C is

$$C = \begin{pmatrix} 0 & C_1^{\text{QT}} & C_1^{\text{TE}} & 0 & C_1^{\text{Td}} & 1 \\ C_1^{\text{TE}} & C_1^{\text{EE}} & C_1^{\text{EE}} & 0 & 0 & C \\ 0 & 0 & 0 & C_1^{\text{BB}} & 0 & C \\ C_1^{\text{Td}} & 0 & 0 & 0 & C_1^{\text{dd}} & C \end{pmatrix} \quad (23)$$

where the diagonal primed elements $C_1^{\alpha X} = C_1^{X X} + N_1^{X X}$ and $X = \text{T;E;B;d}$. In general, $N_1^{\text{EE}} = N_1^{\text{BB}} = 2N_1^{\text{TT}}$. Note that, except for N_1^{dd} , which is not an instrumental noise and emerges only because of the limited reconstruction of the lensing potential by the quadratic estimators of Hu & Okamoto [18], the instrumental noise will increase C , but not its derivatives with respect to the cosmological parameters. This will increase the error on the parameter estimation as seen from Eqs. (20), (22), and (23). It is merely because the instrumental noise dilutes the information below the characteristic beam width scale, and the error increases correspondingly. However, this is not necessarily the case with beam systematics since they couple to the underlying cosmological model, and therefore do depend on cosmological param-

eters. This noise due to systematics, N_1^{sys} , contributes to both C and $\frac{\partial C}{\partial \theta_i}$ and its effect on the confidence level of parameter estimation can be, in principle, either a degradation or an improvement. This argument ignores potential systematic errors, i.e., bias (systematic shift of the average of the statistical distribution which characterizes certain cosmological parameters) of the recovered average values of the cosmological parameters. Indeed, as we show below, the main effect of beam systematics is to bias the inferred cosmological parameters, especially for large beam mismatch parameters, as naively expected (see Fig. 4 for a comparison between the bias and the uncertainty induced on the tensor-to-scalar ratio and neutrino masses by beam ellipticity). It is important to note that, although our focus is on beam systematics and their effect on parameter estimation, we do not include the systematics-induced C_1^{TB} and C_1^{EB} in the analysis (Eqs. 22, 23) because our main concern is how standard data analysis pipelines will be affected by beam systematics. We defer the treatment of the more general case, which includes the parity-violating terms and

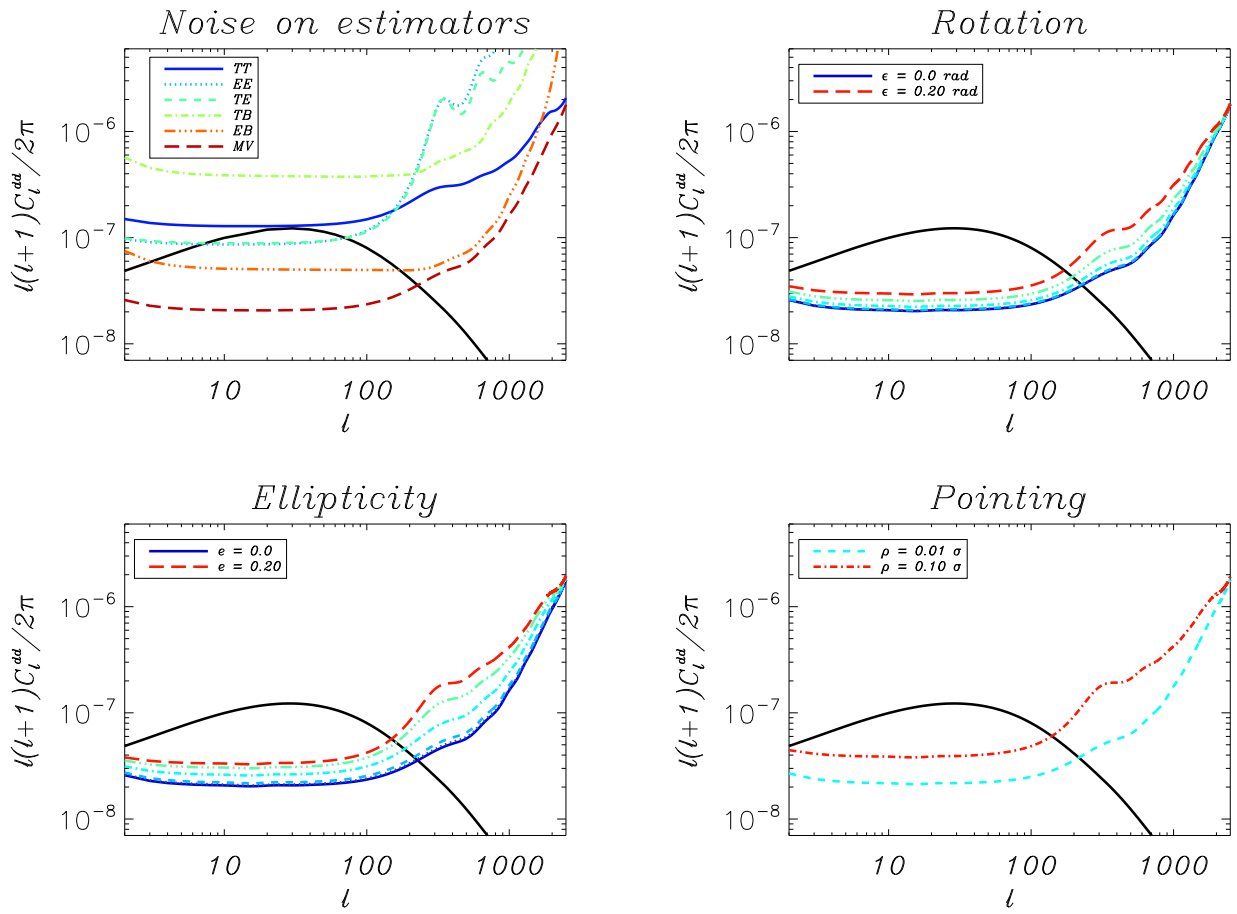


FIG. 3: Lensing reconstruction with QUIET+CLOVER: As in Fig.1. For QUIET+CLOVER sensitivity and angular resolution, the lowest-noise estimator comes from correlations of the TT and TE estimators. Therefore, lensing reconstruction is significantly affected by beam systematics.

their effect on constraints of beyond-the-standard-model parity-violating interactions in the primordial universe, to a future work (Shimon, Miller & Keating [26]).

Given the beam systematics the bias of a parameter can be calculated with the Fisher Matrix. This has been done by O’Dea, Challinor & Johnson [6]. The bias in a parameter θ_i , if not too large, is given by

$$\theta_i = h_i^{\text{obs}} - h_i^{\text{true}} = \sum_j F^{-1}_{ij} B_j \quad (24)$$

where the bias vector B can be written as

$$B = \sum_1^X (C_1^{\text{sys}})^t \frac{\partial C_1^{\text{cmb}}}{\partial \theta_j} \quad (25)$$

and $\theta_{ij} = \text{cov}(C_1^i; C_1^j)$ and C_1 is a vector containing all six power spectra.

Monte Carlo Simulations

The Fisher matrix approach is known to provide reliable approximation to the uncertainty in case of gaussian distributions and only a lower bound for more general distributions by virtue of the Cramér-Rao theorem. It can yield poor estimates, however, in cases of large biases and parameter degeneracies. To check for such effects in our simulations we repeated the analysis with MCMC simulations which make use of the full likelihood function and not only its peak value and can therefore provide reliable estimates of parameter errors even in the presence of large biases. Our simulations illustrate that even when we consider the Fisher-matrix-based results as a guide for choosing the beam parameters for the MCMC simulations, the resulting bias that the Monte-Carlo simulations predict can be much larger than those found with the Fisher-matrix-based calculation (actually Eq. 24 assumes that the bias is small compared to the characteristic width of the likelihood function of the parameter in question; when this is not the case this approximation is

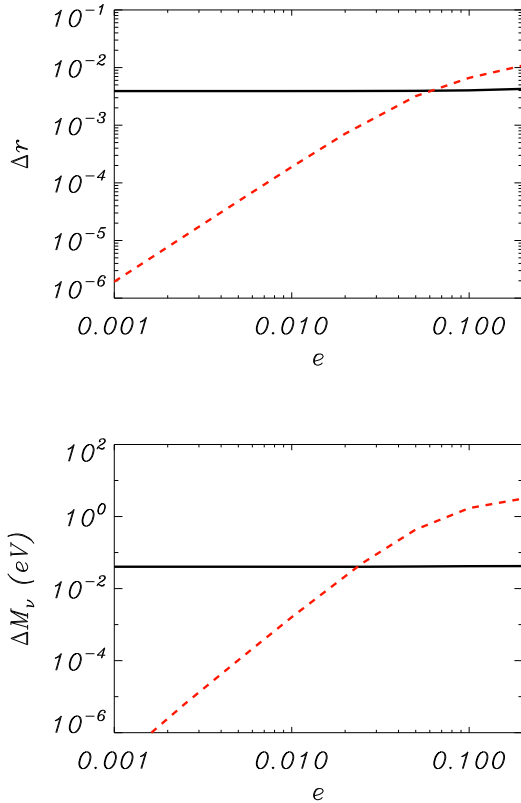


FIG. 4: Uncertainty in the tensor-to-scalar ratio r (top) and total neutrino mass M_ν (bottom) due to beam ellipticity of POLARBEAR. The black solid curve is the statistical error (uncertainty) and the red dashed curve is the bias. As we vary e , the uncertainty increases by only a few percent (i.e. the width of the corresponding 1-D likelihood function does not significantly change). The bias, however, sharply rises with increasing ellipticity, i.e. the expectation value of r and M_ν significantly changes. In general, we find that beam systematics mainly bias the inferred parameters since, for large enough beam systematics parameters, the spurious polarization signal overwhelms the cosmological signal.

invalid) in some cases. This important point is further elucidated in the next section. For our Monte Carlo simulations we use a modified version of CosmoMC [27] which includes measurements of the lensing potential and its cross-correlation with the temperature anisotropy when calculating the likelihood in order to run these simulations. An eleven parameter model is used [$\Omega_b h^2$, $\Omega_{dm} h^2$, Ω_s , w , n_s , n_t , τ , $\log(10^{10} A_s)$, and r]. We ran simulations for each of the five systematic effects with noise corresponding to POLARBEAR, CMBPOL-B and QUIET+CLOVER experiments. While running Monte Carlo simulations is much more time consuming compared to the Fisher matrix approach, the error forecasts for future experiments will ultimately have to account for a potentially significant bias of the inferred cosmologi-

cal parameters.

RESULTS

For both the Fisher and MCMC methods we consider the effect of both irreducible and reducible systematics. By ‘reducible’ we refer to systematics which depend on the coupling of an imperfect scanning strategy to the beam mismatch parameters. These can, in principle, be removed or reduced during data analysis. This includes the differential gain, differential beam width and first order pointing error beam systematics. By ‘irreducible’ we refer to those systematics that depend only on the beam mismatch parameters (to leading order). For instance, the differential ellipticity and second order pointing error persist even if the scanning strategy is ideal. For reducible systematics the scanning strategy is a free parameter in our analysis (under the assumption it is non-ideal, yet uniform, over the map) and we set limits on the product of the scanning strategy (encapsulated by the f_1 and f_2 parameters) and the differential gain, beam width and pointing, as will be described below.

To calculate the power spectra we assume the concordance cosmological model throughout; the baryon, cold dark matter, and neutrino physical energy densities in critical density units $\Omega_b h^2 = 0.021$, $\Omega_c h^2 = 0.111$,

$\Omega_\nu h^2 = 0.006$. The latter is equivalent to a total neutrino mass $M_\nu = \sum_{i=1}^3 m_{\nu_i} = 0.56 \text{ eV}$, slightly lower than the current limit set by a joint analysis of the WMAP data and a variety of other cosmological probes (0.66 eV, e.g. Spergel et al. [28]). We assume degenerate neutrino masses, i.e. all neutrinos have the same mass, 0.19 eV, for the purpose of illustration, and we do not attempt to address here the question of what tolerance levels are required to determine the neutrino hierarchy. As was shown by Lesgourgues et al. [11], the prospects for determining the neutrino hierarchy from the CMB alone, even in the absence of systematics, are not very promising. This conclusion may change when other probes, e.g. Ly-forest, are added to the analysis. Dark energy makes up the rest of the energy required for closure density. The Hubble constant, dark energy equation of state and helium fraction are, respectively, $H_0 = 70 \text{ km sec}^{-1} \text{ Mpc}^{-1}$, $w = -1$ and $Y_{He} = 0.24$. h is the Hubble constant in 100 km/sec/Mpc units. The optical depth to reionization and its redshift are $\tau_{re} = 0.073$ and $z_{re} = 12$. The normalization of the primordial power spectrum was set to $A_s = 2.4 \times 10^9$ and its power law index is $n_s = 0.947$ (Komatsu et al. [24]).

Since the effect of beam systematics is the focus of this paper, and because these systematics are generally manifested on scales smaller than the beam width (except for the effects of differential gain and rotation) we concentrate on some specific cosmological parameters which will be targeted by upcoming CMB experiments. These

parameters have been chosen for our analysis because we expect them to benefit from lensing extraction or simply because they are somehow associated with small angular scales and therefore are prone to systematics on sub-beam scales. We limit our analysis to the tensor-to-scalar ratio r , dark energy equation of state w , spatial curvature Ω_k , running of the scalar index n_s and total neutrino mass M_ν . While r is mainly constrained by the primordial B-mode signal that peaks on degree scales (and is therefore not expected to be overwhelmed by the beam systematics which peak at sub-beam scales), it is still susceptible to the tail of these systematics, extending all the way to degree scales, because of its expected small amplitude (less than 0.1 K). The tensor-to-scalar ratio is also affected by differential gain and rotation which are simply rescalings of temperature anisotropy and E-mode polarization power spectra, respectively, and therefore do not necessarily peak at scales beyond the primordial signal.

The other four parameters either determine the primordial power spectrum $P(k)$ on small angular scales (e.g. n_s) or affect the lensed signal (both temperature and polarization) at late times (e.g. M_ν , Ω_k , w). Ideally, the lensing signal, which peaks at $l \sim 1000$, provides a useful handle on the neutrino mass as well as other cosmological parameters which govern the evolution of the large scale structure and gravitational potentials. However, the inherent noise in the lensing reconstruction process (Hu & Okamoto [18]) which depends, among others, on the instrument specifications (instrumental noise and beam width), now depends on beam systematics as well. The systematics, however, depend on the cosmological parameters through temperature leakage to polarization, and as a result there is a complicated interplay between these signals and the information they provide on cosmological parameters. As our numerical calculations show, the effect on the inferred cosmological parameters stems from both the direct effect of the systematics on the parameters (the top-left 3×3 block of the covariance matrix, Eq. 23) and the indirect effect on the noise in the lensing reconstruction, N_l^{fid} , in cases where the M V estimator is dominated by the EB correlations (see section 3).

Fisher Matrix Results

The Fisher information matrix gives a first order approximation to the lower bounds on errors inferred for these parameters. However, by construction, it uses only the information from the peak of the likelihood function. Markov Chain Monte Carlo simulations are known to be superior to Fisher-matrix-based analysis in cases of strong parameter degeneracies and bias but Fisher matrix results are useful for first order approximation and provide starting values for MCMC simulations. We follow O'Dea, Challinor, & Johnson [6] in quantifying the required tolerance on the differential gain, differential

beam width, pointing, ellipticity and rotation. To estimate the effect of systematics and to set the systematics to a given tolerance limit one has to compare the systematics-free 1- σ error in the i -th parameter (Eq. 20) to the error obtained in the presence of systematics. The latter has two components; the bias and the uncertainty (which depends on the curvature of the likelihood function, i.e. to what extent does the information matrix constrain the cosmological model in question). As in O'Dea, Challinor, & Johnson [6] we define

$$\begin{aligned} &= \frac{\delta_i^0}{\delta_i} j_i^0 \\ &= \frac{\delta_i^0}{\delta_i} j_i^0 \end{aligned} \quad (26)$$

where the superscript 0 refers to values evaluated at the peak of the likelihood function, i.e. the values we assume for the underlying model, and δ_i^0 and δ_i are the bias (defined in Eq. 24) and the change in the statistical error for a given experiment and for the parameters θ_i induced by the beam systematics, respectively. As shown in O'Dea, Challinor, & Johnson [6] these two parameters depend solely on the primordial, lensing and systematics power spectra. We require both δ_i^0 and δ_i not to exceed 10% of the uncertainty without systematics. As illustrated in Fig. 4 for the case of tensor-to-scalar ratio and neutrino total mass, the bias exceeds the uncertainty at some value of the beam ellipticity. This is a general result; for given beam systematic and a cosmological parameter the bias becomes the dominant component of the error in parameter estimation for sufficiently large beam imperfection (ellipticity, gain, etc). This sets the limit on our five systematics parameters as demonstrated in Tables IV, V, VI, VII, VIII and IX for PLANCK, POLARBEAR, SPIDER, QUIET+CLOVER, CMBPOL-A and CMBPOL-B (we considered two cases which we refer to as CMBPOL-A and CMBPOL-B, the former is a high sensitivity experiment with 1000 Planck-equivalent detectors, the latter is motivated by Kaplinghat, Knox & Song [10]) whose specifications are given in Table III. For the systematics power spectra we used the expressions in Table II assuming only temperature leakage (i.e. polarization-free underlying sky) except for the effect of differential rotation where we consider mixing between the E- and B-mode. C^{TE} cannot leak to the B-mode power spectrum since it assumes negative values for certain multipole numbers and C^{E} -contribution is higher order correction to the B-mode systematics and will add only few percent at most to the induced systematics. Due to the scaling of the systematics with the beam width, this potentially negligible C^{E} contribution, which contaminates the B-mode polarization at second order, will result in only a few percent change to the tolerance levels for the beam parameters we consider.

This work is the first to employ Monte-Carlo simulations to assess the effect of beam systematics on parameter estimation. We first considered beam parameters which induce bias in the tensor-to-scalar ratio twice as large as the error (i.e. $\beta = 2$, see Eq. 26) found with the Fisher matrix formalism. For this simulation we selected POLARBEAR, CBPOL-B and QUIET+CLOVER. We focus on the most sensitive cosmological parameters: r , w and M . Our results for POLARBEAR are reported in Table X. The most sensitive parameter to the beam systematics considered here (the beam tolerances set by requiring $\beta = 2$ for $r = 0.01$, a value based on the assumption that the inflation energy scale is associated with the grand unification (GUT) scale, e.g. Bock et al. [29]) turns out to be r , the tensor-to-scalar-ratio. In some cases we found the bias can be as high as 100% for w and M , which are mostly constrained by the larger (compared to the primordial signal from inflation) lensing signal, are changed by no more than 20%, itself a non-negligible bias. Most importantly, we also found that the levels of bias caused by differential beam width and ellipticity exceed the bias found with the naive inclusion of the power spectrum bias in the Fisher-matrix formalism, sometimes by orders of magnitude (Table XIV). This illustrates that the simplistic approach to bias estimation within the Fisher-matrix formalism largely underestimates the induced bias on the cosmological parameters we studied here. However, the Fisher matrix can be used, as done here, to determine the starting values for MCMC simulations. These two systematics, the differential beam width and ellipticity, are second order gradients of the underlying temperature anisotropy as opposed to the first order gradient in case of, e.g. first order pointing error effect. This implies that for given β and ϵ this effect steeply increases towards smaller scales. The Fisher-matrix bias calculation is based, however, on the assumption that the bias is relatively small, an assumption which certainly breaks down when high resolution experiments are considered (i.e. with SPIDER's comparatively low angular resolution, for example, we expect the tension between the Fisher-matrix-based and MCMC estimations of the bias to be smaller). We redone the simulations with tighter constraints on the bias ($\beta = 0.48$ for ellipticity and $\beta = 0.40$ in the case of differential beam width). Again, we used the Fisher matrix results as a starting point. This resulted in significantly reduced biases in the tensor-to-scalar ratio r . Our results are shown in Table XI. Following this analysis we repeated the MCMC simulations with CBPOL-B and QUIET+CLOVER. The results are given in Tables XII and XIII, respectively.

The purpose of this work was to illustrate the effect of beam systematics on parameter extraction from CMB observations. Beam systematics are expected to be significant especially for detecting the B-mode polarization. Ongoing and future experiments must meet very challenging requirements at the experiment design and data analysis phases to assure polarimetric fidelity. Ultimately, a major target of these experiments is the most accurate estimation of cosmological parameters, and for this end it is mandatory to assess, among other issues, the propagation of beam systematics to parameter estimation. The tolerance levels chosen in this work are somewhat arbitrary and may be changed at will, according to the goals of individual experiments, and the numerical values we quote in the tables should be viewed in this perspective.

The only similar work so far to set tolerance levels on beam mismatch in the context of parameter estimation is O'Dea, Challinor & Johnson [6] which influenced our present work. However, we expand on this work in several ways. While O'Dea, Challinor & Johnson [6] considered only the effect of systematics on the tensor-to-scalar ratio r , we consider a family of parameters associated with the B-mode sector: r , M , β , w and κ . We set all other cosmological parameters to be consistent with the WMAP values. In order to exhaust the potential of the CMB to constrain these parameters we carried out lensing extraction. In addition, we repeated the analysis for POLARBEAR, CBPOL-B and QUIET+CLOVER with Monte Carlo simulations and found that the Fisher-matrix approximation is, in general, inadequate for appraising the biases. We also found that high resolution experiments, such as POLARBEAR are very sensitive to bias from second order gradient effects (i.e. differential ellipticity and differential beam width) which is underestimated by the Fisher-matrix-based calculation, but fully accounted for with MCMC simulations. Also, unlike O'Dea, Challinor & Johnson [6] our results are presented independently of the scanning strategy details. The only assumption we made was that the scanning strategy is spatially uniform, a condition which can be achieved with or without a HWP which samples the polarization angles in a way which is uniform; both spatially, and in terms of polarization angle. In case that this approximation fails the more general formalism (Shimon et al. [7]) should be used with the added complexity introduced to lensing reconstruction by the scanning-induced non-gaussianity of the systematic B-mode.

We find that parameter bias is the dominant factor and its level actually sets the upper bounds on the beam parameters appearing in Tables IV through IX. Our results show that the most severe constraints are set on the most sensitive experiments for a given tolerance on β and

since these quantities are experiment-dependent (Eq. 26) and since, in general, an experiment with higher resolution and better sensitivity will result in smaller errors. We expect that the constraints on the systematics should be more demanding so as to realize the potential of experiments. As mentioned above, the most stringent constraints are obtained from the requirement on the bias rather than from increased parameter uncertainty. Again, for the same reason, as shown for specific examples in Fig. 4; the bias always exceeds the uncertainty for large enough systematics and this always takes place before the 10% thresholds in Eqs.(26) are attained. It is also clear from the tables that in general the tensor-to-scalar ratio, r , is the most sensitive parameter, and the second most sensitive is τ , the running of the scalar index (although there are some exceptions). If the tensor-to-scalar ratio is larger than the case we studied ($r = 0.01$), this conclusion may change since r is mainly affected by the overwhelming B-mode systematics on degree scales.

is predicted to vanish by the simplest models of inflation and was added to parameter space to better fit the WMAP and other cosmological data. As is well-known, information from Ly- α systems and other LSS probes can, in principle, better constrain τ if their associated systematics can be controlled to a sufficiently accurate level. For these small scales the CMB is not the ideal tool to extract information and the error that beam systematics induce on τ are not significant.

The upper limits we obtained in this work on the allowed range of beam mismatch parameters for given experiments and given arbitrarily-set tolerance levels on the parameter bias and uncertainty, constitute very conservative limits. It can certainly be the case that some of the systematics studied here may be fully or partially removed. This includes, in particular, the first order pointing error which couples to the dipole moment of non-ideal scanning strategies (see Shimón et al. [7]). By removing this dipole during data analysis the effect due to the systematic first order pointing error (dipole) drops dramatically. We made no attempt to remove or minimize these effects in this work. Our results highlight the need for scan mitigation techniques because the coupling of several beam systematics to non-ideal scanning strategies result in systematic errors. This potential solution reduces systematics, which ultimately propagate to parameter estimation, and affect mainly the parameters considered in this work. A brute-force strategy to idealize the data could be to remove data points that contribute to higher-than-the-monopole moments in the scanning strategy. This would effectively make the scanning strategy 'ideal' and alleviate the effect of the a priori most pernicious beam systematics. This procedure 'costs' only a minor increase in the instrumental noise (due to throwing out a fraction of the data) but will greatly reduce the most pernicious reducible beam systematic, i.e. the first order pointing error (dipole' effect). The bottom line

lesson is clear: the rich treasures of cosmological parameters deducible from B-mode data require a combination of high polarimetric fidelity and judicious data mining. Both are eminently feasible upcoming CMB polarization experiments.

Acknowledgments

We acknowledge the use of the publically available code by Lesgourgues, Perotto, Pastor & Piat for the calculation of the noise in lensing reconstruction. We also used CAMB and CosmoMC for calculations of the Fisher matrices and the Monte Carlo simulations. We acknowledge using resources of the San Diego Supercomputing Center (SDSC). We thank Oliver Zahn for critically reading this paper and for his very useful and constructive suggestions. Useful correspondence with Anthony Challinor is gratefully acknowledged. BK gratefully acknowledges support from NSF PEACASE Award AST-0548262.

-
- [1] Reichardt, C. L., et al. 2008, *ArXiv e-prints*, 801, arXiv:0801.1491
- [2] Zaldarriaga, M., & Seljak, U. 1997, *PRD*, 55, 1830
- [3] Kamionkowski, M., Kosowsky, A., & Stebbins, A. 1997, *Physical Review Letters*, 78, 2058
- [4] Hu, W., Hedman, M. M., & Zaldarriaga, M. 2003, *PRD*, 67, 043004
- [5] Rosset C. et al., arXiv: astro-ph/0410544
- [6] O'Dea, D., Challinor, A., & Johnson, B. R. 2007, *MNRAS*, 376, 1767
- [7] Shim on, M., Keating, B., Ponthieu, N., & Hivon, E. 2008, *PRD*, 77, 083003
- [8] Lewis, A., Challinor, A., & Lasenby, A. 2000, *ApJ*, 538, 473
- [9] Lewis, A., & Bridle, S. 2002, *PRD*, 66, 103511
- [10] Kaplinghat, M., Knox, L., & Song, Y.-S. 2003, *PR*, 91, 241301
- [11] Lesgourgues, J., Perotto, L., Pastor, S., & Piat, M. 2006, *PRD*, 73, 045021
- [12] Perotto, L., Lesgourgues, J., Hannestad, S., Tu, H., & Y Y Wong, Y. 2006, *Journal of Cosmology and Astroparticle Physics*, 10, 13
- [13] Keating, B. G., Keating, B. G. (in preparation). "The Birth Pangs of the Big Bang: An Ultrasonic Image of the Embryonic Universe" in: *VISIONS OF DISCOVERY: New Light on Physics, Cosmology, and Consciousness*, ed. R. Y. Chiao, M. L. Cohen, A. J. Leggett, W. D. Phillips, and C. L. Harper, Jr. Cambridge: Cambridge University Press (arXiv:0806.1781)
- [14] Hanany, S., Hubmayr, J., Johnson, B. R., Matsumura, T., Oxley, P., & Thibodeau, M. 2005, *Applied Optics*, 44, 4666
- [15] Johnson, B. R., et al. 2007, *ApJ*, 665, 42
- [16] MacTavish, C. J., et al. 2007, *ArXiv e-prints*, 710, arXiv:0710.0375
- [17] Zaldarriaga, M., & Seljak, U. 1998, *PRD*, 58, 023003
- [18] Hu, W., & Okamoto, T. 2002, *ApJ*, 574, 566
- [19] <http://lappweb.in2p3.fr/perotto/FUTURCMB/home.html>
- [20] Okamoto, T., & Hu, W. 2003, *PRD*, 67, 083002
- [21] Carroll, S. M. 1998, *Physical Review Letters*, 81, 3067
- [22] Liu, G.-C., Lee, S., & Ng, K.-W. 2006, *Physical Review Letters*, 97, 161303
- [23] Xia, J.-Q., Li, H., Wang, X., & Zhang, X. 2008, *Astronomy & Astrophysics*, 483, 715
- [24] Komatsu, E., et al. 2008, *ArXiv e-prints*, 803, arXiv:0803.0547
- [25] Kosowsky, A., & Loeb, A. 1996, *ApJ*, 469, 1
- [26] Shim on, M., Miller, N., & Keating, B. 2008, work in progress
- [27] <http://cosmologist.info/cosmomic>
- [28] Spergel, D. N., et al. 2007, *ApJS*, 170, 377
- [29] Bock, J., et al. 2006, *ArXiv Astrophysics e-prints*, arXiv:astro-ph/0604101
- [30] <http://www.rssd.esa.int/index.php?project=planck>
- [31] <http://bolb.berkeley.edu/polarbear>

depends on beam substructure	effect	parameter	definition
No	gain	g	$g_1 \quad g_2$
Yes	monopole		$\frac{1 - z}{1 + z}$
Yes	dipole		$1 \quad 2$
Yes	quadrupole	e	$\frac{x - y}{x + y}$
No	rotation	"	$\frac{1}{2} ("_1 + "_2)$

TABLE I: Definitions of the parameters associated with the systematic effects. Subscripts 1 and 2 refer to the first and second polarized beams of the dual-beam polarization assumed in this work.

effect	parameter	C_1^{TE}	C_1^E	C_1^B
gain	g	0	$g^2 f_1 ? C_1^T$	$g^2 f_1 ? C_1^T$
monopole		0	$4^{-2} (l)^4 C_1^T ? f_1$	$4^{-2} (l)^4 C_1^T ? f_1$
pointing		$c J_1^2 (l) C_1^T ? f_3$	$J_1^2 (l) C_1^T ? f_2$	$J_1^2 (l) C_1^T ? f_2$
quadrupole	e	$I_0 (z) I_1 (z) c C_1^T$	$I_1^2 (z) c^2 C_1^T$	$I_1^2 (z) s^2 C_1^T$
rotation	"	0	$4^{-2} C_1^B$	$4^{-2} C_1^E$

TABLE II: The scaling laws for the systematic effects to the power spectra C_1^T , C_1^{TE} , C_1^E and C_1^B assuming the underlying sky is not polarized (except for the rotation signal where we assume the E, and B-mode signals are present) and a general, not necessarily ideal or uniform, scanning strategy. The next order contribution (10% of the 'pure' temperature leakage shown in the table) is contributed by C_1^{TE} . It can be easily calculated based on the general expressions in Shim on et al. [7] where the definitions of z , c , s , etc., are also found. For the pointing error we found that the 'irreducible' contribution to B-mode contamination, arising from a second order effect, is extremely small and therefore only the first order terms (which vanish in ideal scanning strategy) are shown. The functions f_1 and f_2 are experiment-specific and encapsulate the information about the scanning strategy which couples to the beam mismatch parameters to generate spurious polarization. In general, the functions f_1 and f_2 are spatially-anisotropic but for simplicity, and to obtain a first-order approximation, we consider them constants (see sec. 2.2) in general. In the case of ideal scanning strategy they identically vanish. The exact expressions are given in Shim on et al. [7].

Experiment	f_{sky}	ν	b	τ	E
PLANCK	0.65	30	33'	2.0	2.8
		44	24'	2.7	3.9
		70	14'	4.7	6.7
		100	9.5'	2.5	4.0
		143	7.1'	2.2	4.2
		217	5.0'	4.8	9.8
		353	5.0'	14.7	29.8
		545	5.0'	147	1
		857	5.0'	6700	1
POLARBEAR	0.03	90	6.7'	1.13	1.6
		150	4.0'	1.70	2.4
		220	2.7'	8.0	11.3
SPIDER	0.6	96	58'	0.46	0.65
		145	40'	0.50	0.71
		225	26'	2.22	3.14
		275	21'	5.71	8.08
QUIET+CLOVER	0.015	150	10'	0.34	0.48
CMBPOL-A	0.65	150	5'	0.22	0.32
CMBPOL-B	0.65	150	3'	1.0	1.4

TABLE III: Instrumental characteristics of the CMB polarimeters considered in this work: f_{sky} is the observed fraction of the sky, ν is the center frequency of the channels in GHz, b is the FWHM (Full Width at Half Maximum) in arc-minutes, τ is the temperature sensitivity per pixel in K and $E = \frac{\tau}{b}$ is the polarization sensitivity. For all experiments, we assumed one year of observations (PLANCK [30], POLARBEAR [31], SPIDER [16], QUIET+CLOVER [6]). CMBPOL A & B represent toy experiments for illustration with CMBPOL-A having 1000 PLANCK detectors and PLANCK resolution and CMBPOL-B has higher resolution but 1 K noise level (Kaplighat, Knox & Song [10]).

Parameter	Nominal value	$\frac{g}{1\%} \sqrt{\frac{f_1}{2}}$	$\frac{w}{1\%} \sqrt{\frac{f_1}{2}}$	$(\frac{1}{1\%}) \sqrt{\frac{f_2}{2}}$	$\frac{e}{1\%}$	" [deg]
r	0.01	0.02	0.42	1.5	0.8	0.72
w	-1	0.33	0.38	2.5	2.4	2.86
k	0	0.37	0.44	3.0	2.6	3.72
	0	0.67	0.33	2.2	2.1	2.23
M [eV]	0.56	0.32	0.38	2.4	2.4	2.58

TABLE IV: Systematics tolerance for PLANCK: shown are the nominal cosmological parameters we used along with the tolerance levels (as defined by the criterion that both g and w , Eq. 26, should not exceed the 10% threshold) set on combinations of the quadrupole of the scanning strategy (f_1 , under the assumption of uniform scanning strategy) and the dimensionless differential gain g and differential beam width w . Also is shown the constraint on pointing error weighted by the dipole of the scanning strategy (f_2) in arcsec units. The tolerance level on ellipticity e is dimensionless (we assumed the worst-case scenario that $\theta = 45^\circ$) and the allowed rotation " is given in angular degrees. Except for the differential beam width effect, the most severe constraints are obtained from the requirement that r is not biased. g and w , the parameters representing the differential gain and differential beam width, are defined in Table I.

Parameter	Nominal value	$\frac{g}{1\%} \sqrt{\frac{f_1}{2}}$	$\frac{w}{1\%} \sqrt{\frac{f_1}{2}}$	$(\frac{1}{1\%}) \sqrt{\frac{f_2}{2}}$	$\frac{e}{1\%}$	" [deg]
r	0.01	0.01	0.74	0.5	1.4	0.25
w	-1	0.16	0.38	1.7	1.8	1.26
k	0	0.18	0.39	1.8	1.8	2.01
	0	0.17	0.30	1.2	1.3	0.77
M [eV]	0.56	0.15	0.42	1.9	1.8	1.06

TABLE V: Systematics tolerance for POLARBEAR: As in Table IV.

Parameter	Nominal value	$\frac{g}{1\%} \sqrt{\frac{f_1}{2}}$	$\frac{1}{1\%} \sqrt{\frac{f_1}{2}}$	$(\frac{1}{1\%}) \sqrt{\frac{f_2}{2}}$	$\frac{e}{1\%}$	" [deg]
r	0.01	0.03	0.10	2.2	0.19	0.97
w	-1	0.13	0.31	9.2	0.47	2.86
k	0	0.10	0.57	9.9	1.75	3.43
	0	0.19	0.12	5.9	0.55	6.88
M [eV]	0.56	0.10	0.26	10.9	0.38	3.72

TABLE V I: Systematics tolerance for SPIDER : A s in Table IV .

Parameter	Nominal value	$\frac{g}{1\%} \sqrt{\frac{f_1}{2}}$	$\frac{1}{1\%} \sqrt{\frac{f_1}{2}}$	$(\frac{1}{1\%}) \sqrt{\frac{f_2}{2}}$	$\frac{e}{1\%}$	" [deg]
r	0.01	0.009	0.20	0.4	0.4	0.4
w	-1	0.114	0.17	3.2	0.6	1.8
k	0	0.122	0.18	3.5	0.7	2.1
	0	0.148	0.13	1.4	0.4	1.3
M [eV]	0.56	0.109	0.18	3.1	0.7	1.7

TABLE V II: Systematics tolerance for QUIET + CLOVER : A s in Table IV .

Parameter	Nominal value	$\frac{g}{1\%} \sqrt{\frac{f_1}{2}}$	$\frac{1}{1\%} \sqrt{\frac{f_1}{2}}$	$(\frac{1}{1\%}) \sqrt{\frac{f_2}{2}}$	$\frac{e}{1\%}$	" [deg]
r	0.01	0.0016	0.05	0.04	0.10	0.023
w	-1	0.0259	0.19	0.4	0.28	0.773
k	0	0.0270	0.21	0.4	0.28	0.372
	0	0.0266	0.08	0.3	0.21	0.123
M [eV]	0.56	0.0251	0.18	0.4	0.28	0.401

TABLE V III: Systematics tolerance for CMBPOL-A : A s in Table IV .

Parameter	Nominal value	$\frac{g}{1\%} \sqrt{\frac{f_1}{2}}$	$\frac{1}{1\%} \sqrt{\frac{f_1}{2}}$	$(\frac{1}{1\%}) \sqrt{\frac{f_2}{2}}$	$\frac{e}{1\%}$	" [deg]
r	0.01	0.0031	0.57	0.2	1.1	0.066
w	-1	0.0728	0.40	0.9	1.7	0.716
k	0	0.0762	0.39	0.8	1.8	0.888
	0	0.0600	0.30	0.4	1.3	0.315
M [eV]	0.56	0.0700	0.45	1.4	1.7	0.544

TABLE IX : Systematics tolerance for CMBPOL-B : A s in Table IV .

Parameter	no sys.		di . gain		di . pointing		di . rotation	
r	0:0100	0:0039	0:0210	0:0046	0:0230	0:0058	0:0220	0:0050
w	1:20	0:32	1:12	0:32	1:26	0:31	1:20	0:32
M [eV]	0:56	0:06	0:54	0:06	0:58	0:06	0:56	0:06

TABLE X : The effect of differential gain, pointing and rotation on parameter estimation for POLARBEAR obtained with MCMC simulations. The systematic beam parameters ϵ , g , etc. were chosen so that $\epsilon = 2$ (Eq.26), i.e. the bias is twice as large as the uncertainty in the tensor-to-scalar ratio r (assuming $r = 0.01$), as obtained by the Fisher-matrix-based calculation ($\frac{g}{1\%} \sqrt{\frac{f_1}{2}} = 0.05$, $\frac{1}{1\%} \sqrt{\frac{f_2}{2}} = 2.6$, $\epsilon = 1.2$). The values shown are the cosmological parameters recovered from the full likelihood function and their 1- σ errors. The biases we obtain for differential beam width and ellipticity are orders of magnitude larger and are not shown here.

Parameter	no sys.		di. beam width		di. ellipticity	
r	0:0100	0:0039	0:0120	0:0042	0:013	0:0043
w	1:22	0:31	1:35	0:28	1:19	0:30
M [eV]	0:56	0:07	0:66	0:06	0:56	0:06

TABLE XI: The effect of differential beam width and ellipticity on parameter estimation from POLARBEAR obtained with using MCMC simulations. The beam parameters g , e , etc. were chosen so that $\theta = 0.40$ and 0.48 , respectively (Eq.26), as obtained by the Fisher-matrix-based calculation ($\sqrt{\frac{f_1}{2}} = 1.6\%$, $e = 3.5\%$).

Parameter	no sys.		di. gain		di. pointing		di. beam width		di. ellipticity		di. rotation	
r	0:0100	0:00037	0:01090	0:00044	0:0110	0:0046	0:01100	0:00045	0:011	0:00049	0:01100	0:00039
w	1:04	0:09	0:910	0:097	1:11	0:12	1:6	0:11	1:11	0:11	1:11	0:11
M [eV]	0:54	0:01	0:52	0:02	0:56	0:02	0:63	0:01	0:56	0:02	0:56	0:02

TABLE XII: The effect of beam systematics on parameter estimation from CMBPOL-B obtained with using MCMC simulations. Here $g = 0.014\sqrt{\frac{f_1}{2}}\%$, $\theta = 2.78\sqrt{\frac{f_1}{2}}\%$, $\theta = 0.64''\sqrt{\frac{f_2}{2}}$, $e = 5\%$ (with $\theta = 45^\circ$) and $\psi = 19^\circ$.

Parameter	no sys.		di. gain		di. pointing		di. rotation	
r	0:010	0:003	0:0200	0:0041	0:0280	0:0068	0:0220	0:0048
w	1:15	0:37	1:12	0:35	1:16	0:34	1:15	0:34
M [eV]	0:55	0:01	0:54	0:09	0:58	0:10	0:57	0:10

TABLE XIII: The effect of beam systematics on parameter estimation from QUIET+CLOVER obtained with using MCMC simulations. Here $g = 0.046\sqrt{\frac{f_1}{2}}\%$, $\theta = 3.2\sqrt{\frac{f_1}{2}}\%$, $\theta = 2.3''\sqrt{\frac{f_2}{2}}$, $e = 4.4\%$ (with $\theta = 45^\circ$) and $\psi = 2.1^\circ$.

Experiment	Beam parameter	r from MCMC
POLARBEAR	$g\sqrt{\frac{f_1}{2}}$	2.8
	$\sqrt{\frac{f_2}{2}}$	3.3
	$\sqrt{\frac{f_1}{2}}$	0 (100)
	e	0 (100)
	"	3.1
CMBPOL-B	$g\sqrt{\frac{f_1}{2}}$	2.4
	$\sqrt{\frac{f_2}{2}}$	2.7
	$\sqrt{\frac{f_1}{2}}$	2.7
	e	2.7
	"	2.7
QUIET+CLOVER	$g\sqrt{\frac{f_1}{2}}$	3.3
	$\sqrt{\frac{f_2}{2}}$	6.00
	$\sqrt{\frac{f_1}{2}}$	0 (100)
	e	0 (100)
	"	4.0

TABLE XIV: The bias in the tensor-to-scalar ratio r (r_r) obtained with MCMC for POLARBEAR, CMBPOL-B and QUIET+CLOVER. These r_r values were obtained by assuming each of the five systematics we considered have the values which induce a bias $r_r = 2$ in the Fisher matrix analysis. This table is a compilation of the corresponding values for r reported in Tables X, X II and X III. Note the significant discrepancy between the Fisher-matrix-based and MCMC forecast for the bias for the differential beam width and ellipticity systematics. Both scale as the second-order gradient of the temperature C_1^{sys} / C_1^T and as a result of this steep rise of the systematics with scale the systematics soon overwhelm the primordial B-mode signal and significantly bias the deduced tensor-to-scalar ratio. The Fisher matrix estimate of the bias is only a leading order approximation in case the bias is small; an assumption which evidently does not apply to systematics which scale as the second order gradient of the temperature anisotropy.